MICROWAVE REMOTE SENSING OF ATMOSPHERIC WATER PARAMETERS

Kristina B. Katsaros
Dept. of Atmospheric Sciences
University of Washington
Seattle, WA 98195
(206) 543-1203

1. ABSTRACT

The Scanning Multichannel Microwave Radiometers (SMMR's) and the Special Sensor Microwave/Imager (SSM/I), operated from polar orbiting satellites, provide measurements of atmospheric water parameters in the form of integrated atmospheric water vapor (IWV), integrated cloud liquid water (ICLW), rain and the presence of graupel or other large ice particles in the clouds over the oceans of the earth. At the University of Washington, we have used this relatively new resource in mesoscale studies of mid-latitude cyclonic storms and tropical cloud clusters. Some of our findings are: position of fronts in mid-latitude cyclones can be accurately located using the pattern in integrated water vapor. Areal coverage of rain in tropical cloud clusters can be measured, while determination of rain rate may require further algorithm development. Combining passive microwave information with scatterometer derived convergence patterns gives insights into storm structure and dynamics. Cloud water and rain data derived from microwave signals can be used to verify parameterizations of these quantities in limited area numerical models.

2. INTRODUCTION

Data on moisture are useful for diagnosing and predicting both thermo-dynamic and dynamic properties of the atmosphere. Radiosonde ascents and infrared and microwave satellite sounders provide temperature and humidity profiles, and visible and infrared images from

satellites provide location of cloud masses. However, over oceanic regions very few radiosonde stations exist, being limited to weather ship and island stations. Visible and infrared techniques do not give information below cloud tops. Microwave sounders provide some humidity information in the presence of clouds, even though still not of very high vertical or horizontal resolution. Thus, satellite-borne sensors, which can provide relevant measures of atmospheric water content (as vapor, cloud water, rain or ice particle concentration) could fill an important data gap. Passive microwave sensors operating at window frequencies greater than 18 GHz can provide these atmospheric water parameters. They are still only available at somewhat low horizontal resolution and only provide integrated values over the whole atmospheric column, but they provide a unique view of atmospheric storms over the ocean.

How atmospheric water vapor and cloud water can be deduced by microwave remote sensing was described by Staelin et al. (1976). Buettner (1963) appears to have been first to suggest that rain could be observed over the ocean using microwave radiometers with wavelengths of the order of 1 cm. He based his speculation on an early report of Mie-calculations of extinction by polydisperse media (such as rain) at microwave wavelengths (Deirmendjian, 1963; see also Deirmendjian, 1968).

Information on atmospheric water in its various forms over the ocean obtained by microwave radiometry from space has been available for research since the mid-1970's. Parameters which are derived include integrated atmospheric water vapor (IWV), integrated cloud liquid water (ICLW) and rain rate (or rain occurrence). The two most recent types of instruments providing these data are the Scanning Multichannel Microwave Radiometer (SMMR) operating on Seasat for 3 months in 1978, and on Nimbus 7, from October 1978 until the fall of 1987 - and the Special Sensor Microwave/Imager (SSM/I), launched on the F8 satellite in the U.S. Defense Meteorological Satellite Program (DMSP) in June of 1987.

Characteristics of the SMMR and SSM/I and the algorithms used to calculate the atmospheric water parameters are described in Section 3. Research on mid-latitude cyclones and tropical

cloud clusters, performed with SMMR data at the University of Washington, is summarized in Section 4 and the promising synergy which develops when data from a scatterometer or numerical models are combined with microwave radiometer data is discussed in Sections 5 and 6, followed by conclusions and a look to the future in Section 7.

3. INSTRUMENTS AND ALGORITHMS

The frequencies employed by the two microwave instruments discussed here, the SMMR and the SSM/I are listed in Table 1. The SMMR instrument has been described by Gloersen and Barath (1977) and the SSM/I by Hollinger et al. (1987).

Table 1. ***Characteristics of the Two Polar Orbiting Radiometers - SMMR on Seasat and on Nimbus 7 and the SSM/I on the F8 DMSP Satellite***

SMMR		SSM/I	
FREQ. GHz	APPROX. RESOLUTION (km)	FREQ. GHz	APPROX. RESOLUTION (km)
6.6	150	--	--
10.7	100	--	--
18	65	19.35	55
21	60	22.235	50
37	35	37	35
--	--	85.5	15
Swath Width: Seasat: 650 km; Nimbus 7: 780 km		*Swath Width:* 1400 km	
Period of Operation: Seasat: July-October1978; Nimbus 7: October 1978-Fall, 1987		*Period of Operation:* July, 1987 - Present	

Because microwave wave-lengths are relatively long, antennae of reasonable size can only provide horizontal resolution on the earth's surface of 10 to 100 km dependent on wavelength.

Since the emissivity of the sea is only about 0.5, its brightness temperatures is about 150°K. Against this cold and relatively uniform background, satellite sensors measure the stronger signals from atmospheric water vapor, cloud liquid water and rain. Water vapor is measured primarily by frequencies in a weak absorption line around 22 GHz. The SMMR operates at 21 GHz on the longwave flank of the line, while the SSM/I senses the center of this line. The resolution at these relatively low frequencies is about 50 km x 50 km. The water vapor algorithms are well founded. Therefore, all tests of IWV data from the two SMMR's give bias values and standard deviations which are comparable to those of the operational radiosondes (Katsaros et al., 1981; Alishouse, 1983; Chang et al., 1984; Gloersen et al., 1984; McMurdie, 1988). An example taken from the latter reference is seen in Figure 1.

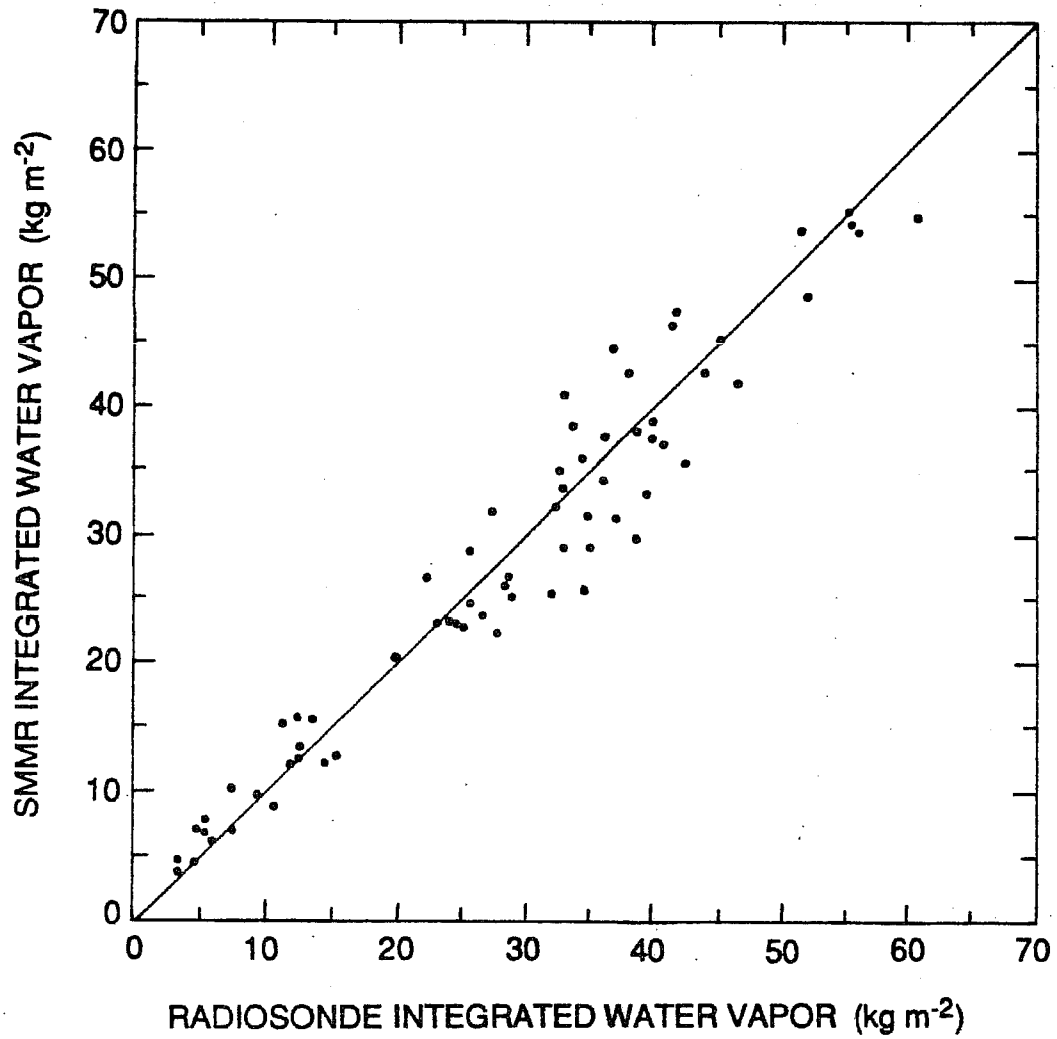

Figure 1: Integrated water vapor calculated from radiosonde information from island and ship stations located in the tropics, midlatitudes and high latitudes vs. integrated water vapor derived from SMMR for the year 1979. Only SMMR passes within ±2 hrs. of the radiosonde launch and within a 1° latitude/longitude radius of the station were selected. 70 matchups were used for this figure. SMMR values have an r.m.s. difference of 2.7 kg m^{-2} from the radiosonde values (after McMurdie, 1988).

The present evidence is that a recent IWV algorithm for SSM/I does equally well (Alishouse, 1988, personal communication).

Algorithms for calculating integrated cloud liquid water and/or rain rate from SMMR signals have been proposed by Wilheit and Chang (1980), Spencer, (1986), Olson (1987), and Petty and Katsaros (1988). Unfortunately, integrated cloud liquid water and rain determinations are much harder to verify than IWV, particularly over the oceans. McMurdie and Katsaros (1985) and Katsaros and Lewis (1986) found that the ICLW derived from the theoretical algorithms showed qualitatively good agreement with the occurrence of clouds in satellite visible or infrared images. A particularly convincing example is found in the article by Katsaros and Lewis, where a dry-slot ahead of a North Pacific cold front is captured by the SMMR data (even though the instrument brightness temperatures were not fully corrected for biases). During one flight with an instrumented aircraft during the STREX (Storm Transfer Response Experiment) in December 1980, a warm-frontal deep nimbostratus cloud was sampled by a spiral flight over a period of one hour. Integration of a Johnson-Williams cloud water sampler and of the dropsize distributions from Knollenberg droplet counters gave identical values for the ICLW in the column, 0.4 kg/m^2, which coincided exactly with the value calculated from the Nimbus 7 SMMR in the general vicinity. This is a rare example of such coincidence.

Rain rates calculated from SMMR over the ocean have been compared to qualitative ship reports (McMurdie and Katsaros, 1985), to coastal rain gauges (Katsaros and Lewis, 1986) and to rain rates derived from coastal radar measurements (e.g., Spencer et al., 1983a; Spencer, 1986; and Petty and Katsaros, 1988). For mid-latitude cyclones, where the rain rates are relatively low, the agreement appears to be very good, of the order of a factor of two. In several other publications Spencer and collaborators have evaluated interpretation of SMMR signals in terms of rain rate over intense continental convective storms (e.g., Spencer et al. 1983b, 1983c; Spencer, 1984; Spencer and Santek, 1985). These articles also claim reasonable agreement with radar measurement.

Except for the 85 GHz channels on the SSM/I, which have a 12 km x 12 km resolution, the resolution elements available from SMMR or SSM/I are much larger than many interesting precipitation features of atmospheric weather systems. In particular, rain bands and convective rain cells often occur on scales between a few to tens of km. Because of non-linearities in the relationship between rain rate and microwave emission, an areal average over the footprint of the satellite instrument does not properly represent the true average rain rate over that area in such cases. If the whole rain cell has rain rates > 5 mm/hr. algorithms based on 37 GHz emission signals have reached an assymtotic limit and even become double valued. Figure 2 from Wilheit et al. (1977) illustrates this point. Algorithms based on scattering from the hydrometeors occurring as ice (graupel or snow) appear to better represent the rain rate in intense convective storms over oceans as well as over land (e.g., Spencer, 1986).

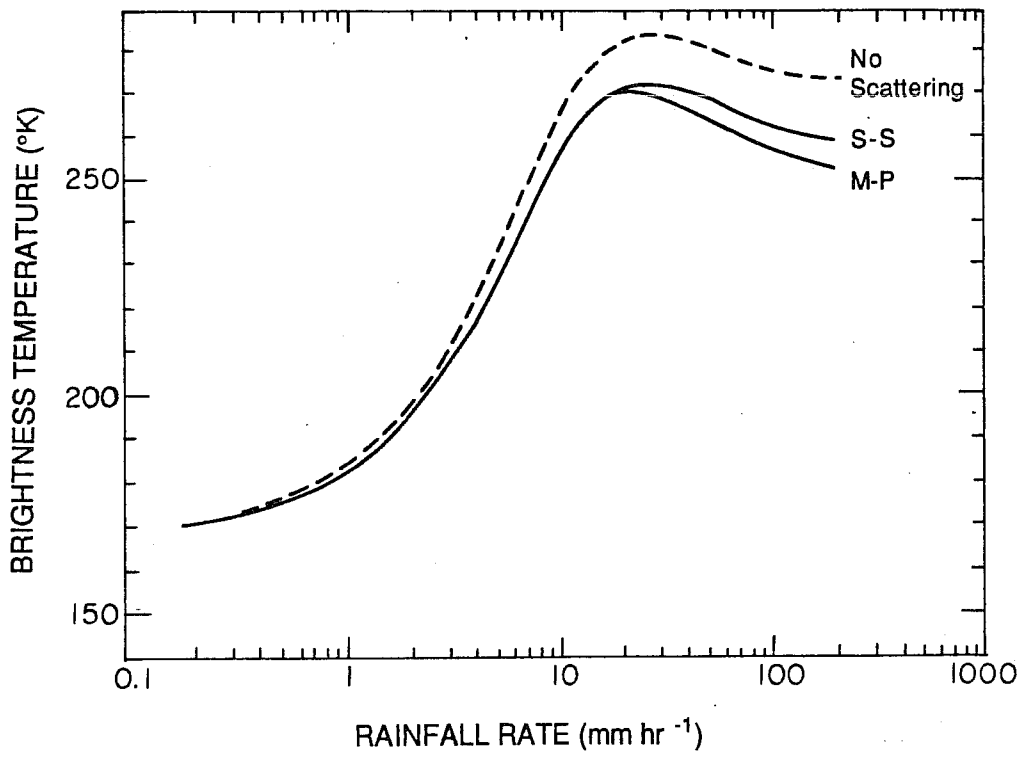

Figure 2: Calculated brightness temperature at 1.55 cm (19.35 GHz) as a function of rain rate with scattering included in the model (solid lines) and excluded from the model (dashed line). In both cases, the assumed freezing level is 4 km. The M-P and S.S. designations specify the Marshall-Palmer and Sekhon-Srivastava particle size distributions, respectively (after Wilheit, et al., 1977).

4. STUDIES OF WEATHER SYSTEMS ON MESOSCALE TO GLOBAL SCALE

4.1 Mid-Latitude Cyclones

In spite of the limitations in resolution and sampling frequency, studies employing microwave data from space illustrate that a valuable new resource for diagnosing mid-latitude atmospheric weather systems has been developed (Taylor et al., 1981, 1983; McMurdie and Katsaros, 1985; Katsaros and Lewis, 1986; Spencer et al., 1983a; McMurdie et al., 1987; Katsaros et al., 1989). McMurdie and Katsaros (1985) found that a definitive relationship existed between patterns in integrated atmospheric water vapor (IWV) and the surface location of fronts in mid-latitude cyclones. Figure 3 is an illustration of this relationship during a typical life-cycle of a North Pacific winter time cyclone.

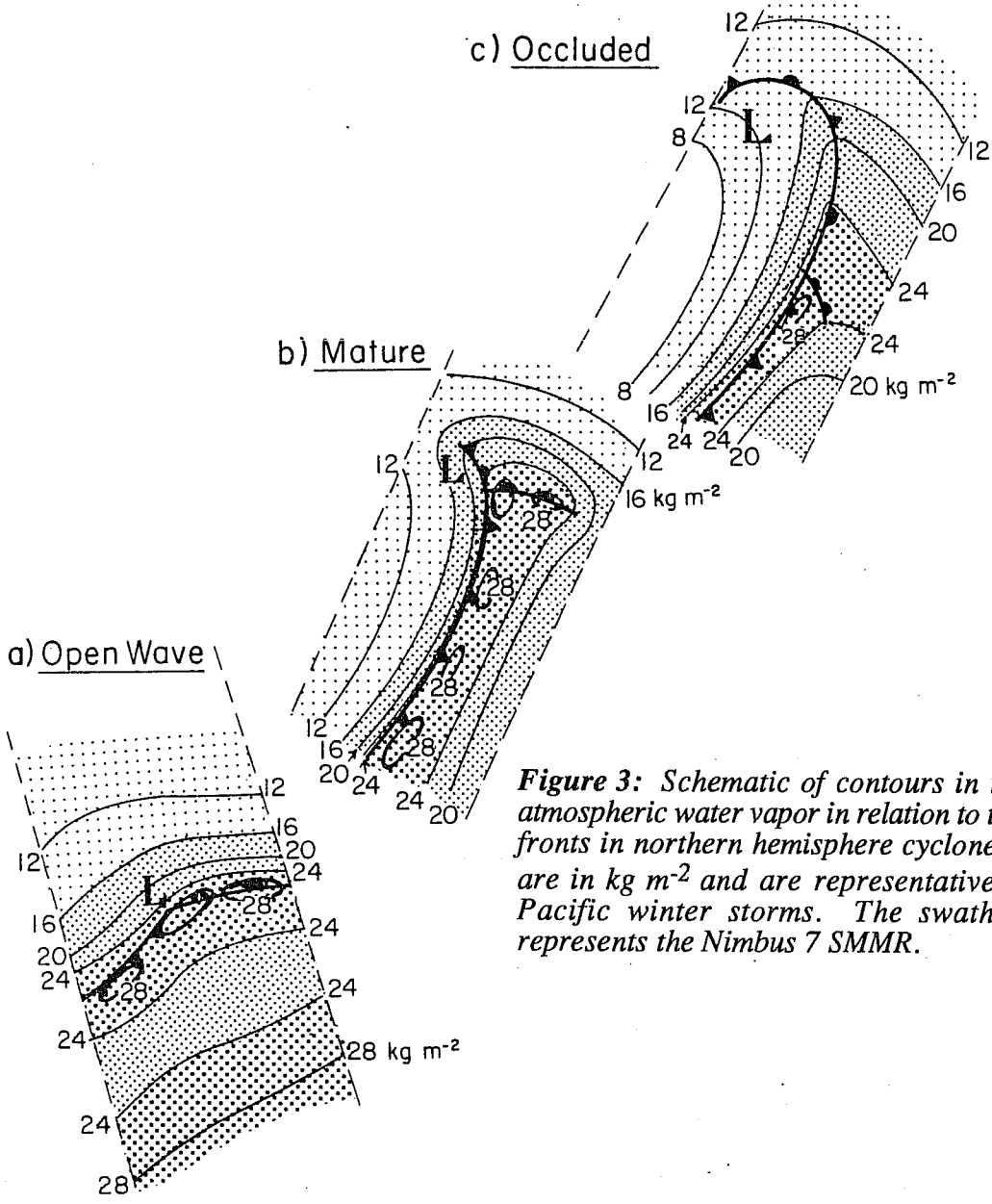

Figure 3: *Schematic of contours in integrated atmospheric water vapor in relation to the surface fronts in northern hemisphere cyclones. Values are in kg m^{-2} and are representative of North Pacific winter storms. The swath sampled represents the Nimbus 7 SMMR.*

Examining many cyclones with the Nimbus 7 SMMR IWV data, McMurdie (1988) found statistical differences between the maximum and minimum IWV associated with cold fronts in different seasons and regions of the global ocean. In spite of that, Katsaros, et al. (1989) found that the same numerical threshold value for the gradient in IWV accurately locates fronts in all seasons and over all oceans, from the Southern Ocean to the North Pacific and North Atlantic. In the latter reference a flag based on this threshold was calculated. It was found to outline cold and warm fronts in 87% of the 65 cases studied. Rain occurrence based on a simple flagging routine was also found to be a dependable locator of frontal zones (in 91% of the cases). The two measures do not capture exactly the same features. The water vapor gradient flag is particularly good at outlining the location of cold fronts away from the central depression, while the rain flag generally maps the region near the apex of the frontal wave. Figure 4 shows an example from the Southern Hemisphere, where this technique could possibly make a valuable contribution. (However, the location of the front in Figure 4 is that produced by the Australian Weather Service which illustrates that information currently available operationally often is quite adequate).

Mesoscale features such as rain bands, waves on fronts, dry slots and convective regions within large cloud masses behind cold fronts or occluded fronts can be discerned in SMMR data, which might be very valuable for short-range forecasting. Several examples of such features are seen in the articles by McMurdie and Katsaros (1985), Katsaros and Lewis (1986), McMurdie et al. (1987) and Katsaros et al. (1989) from which Figure 5 shows a few examples. Figures 4, 8 and 9 have additional examples from mid-latitude cyclones.

4.2 Tropical Cloud Clusters

During the Winter MONEX (Monsoon Experiment) in December 1978, the Massachusetts Institute of Technology operated a radar at Bintulu on Borneo. Data on rain rate derived from these radar signals, seaward of Bintulu, provide an opportunity to compare rain estimates derived from the Nimbus 7 SMMR for tropical cloud clusters to surface based measurements (Petty and Katsaros, 1988). A polarization based rain algorithm employing the two 37 GHz channels was used in this study.

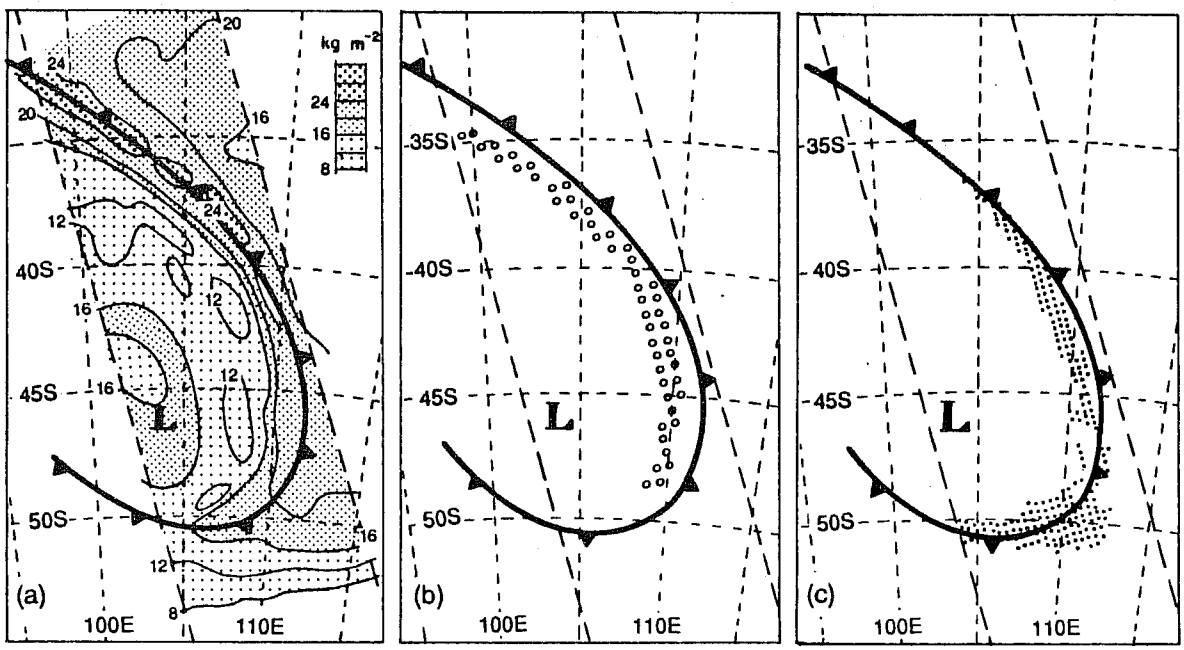

Figure 4: Identification of a frontal location in the Southern Hemisphere by a water vapor gradient flag and a rain occurrance flag (after Katsaros, et al., 1989). This case was sampled by Nimbus 7 SMMR on January 14, 1979 at 05:19 UCT, Orbit #1133.

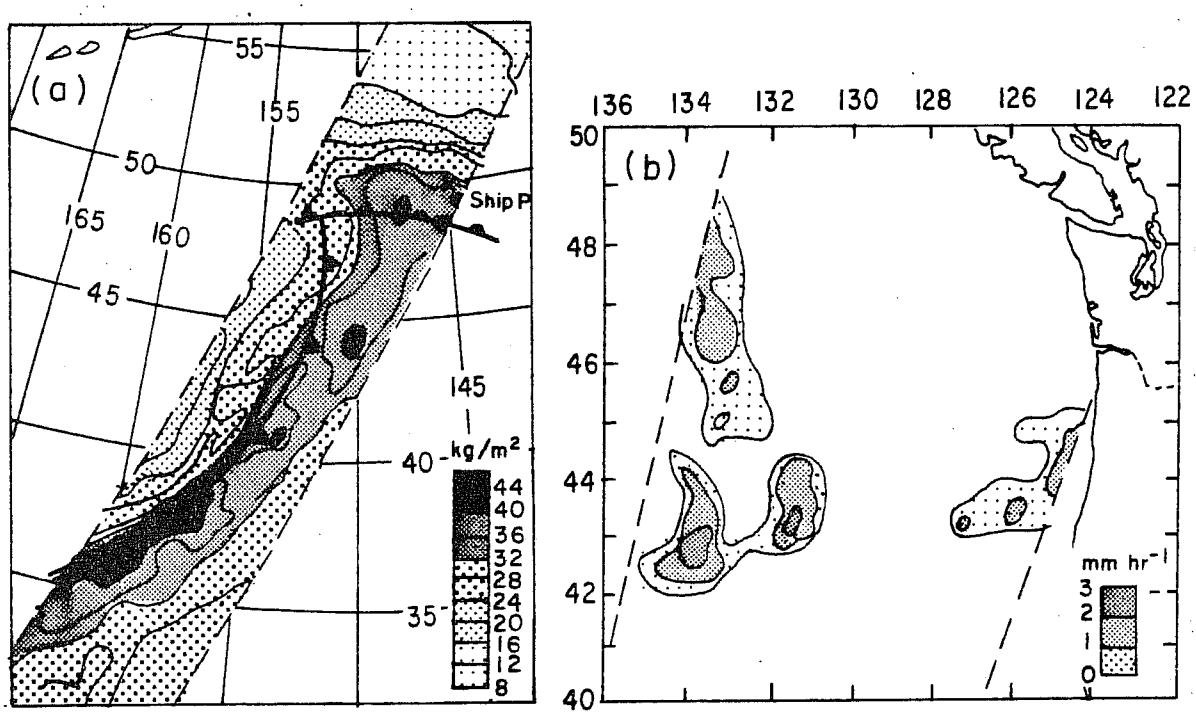

Figure 5: Examples of mesoscale features identified in SMMR data.

a) A frontal wave seen in the horizontal distribution of integrated water vapor in a North Pacific Storm at 0900 UTC on September 11, 1978, Seasat SMMR (after McMurdie and Katsaros, 1985).

b) Convective rain areas identified in the area behind a cold front off the U.S. West coast at 0105 PST on March 5, 1979, Nimbus 7 SMMR (after Katsaros and Lewis, 1986).

During the course of the work it became clear that the rain in tropical cloud clusters saturates the 37 GHz signals most of the time so that no differentiation is possible within heavily raining clouds. Instead the data are a better indicator of areal coverage by rain. It appears that due to saturation one loses about two-thirds of the true rain rate. An empirical correction which would allow quantitative rain rate estimates, could probably be developed, when a larger data base becomes available. Possibly, information on the stage of development of the cloud cluster determined from visible or infrared satellite measurements, as suggested by Adler and Negri (1988), could be folded into the microwave algorithm for greater specificity.

Figures 6 and 7, taken from Petty and Katsaros (1988), illustrate the correlation with operational infrared imagery and the difference in resolution between surface based radar data and the SMMR footprint at 37 GHz respectively.

5. COMBINING SCATTEROMETER AND SMMR DATA

On the experimental Seasat satellite there were several other microwave instruments besides the SMMR (Born et al., 1979). Among them was the Seasat scatterometer, SASS, an active microwave instrument, which sends out a radar signal from two antennas at 90° angles to each other. The backscattered return signals are a measure of the sea surface roughness on a small scale (about 5 cm), which is closely related to the near surface wind stress or wind speed. Because of asymmetry in the backscatter downwind and crosswind, the signals can be interpreted to give wind direction as well as speed. Much work has been done in evaluating the accuracy of these complex signals and interpreting them (e.g., Wurtele et al., 1982). Levy and Brown (1986) have developed a practical method to calculate wind fields at 50 km resolution from which the divergence field can be obtained. Since Seasat carried both a SMMR and a scatterometer, these surface layer divergence fields can be correlated with SMMR IWV fields and rain regions. Such comparisons were made by McMurdie et al. (1987). One expects that regions of large water vapor content and rain would be correlated with surface convergence and the consequent vertical motion. An example case during the Queen Elizabeth II storm, is presented in Figure 8. It is clear that the information from the two satellite instruments support each other and lend credence to both sets of algorithms.

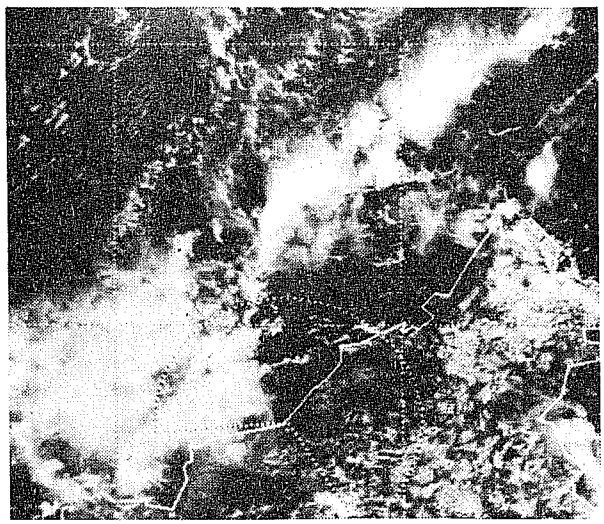

(a) GMS - 1 Visible 0233 UTC

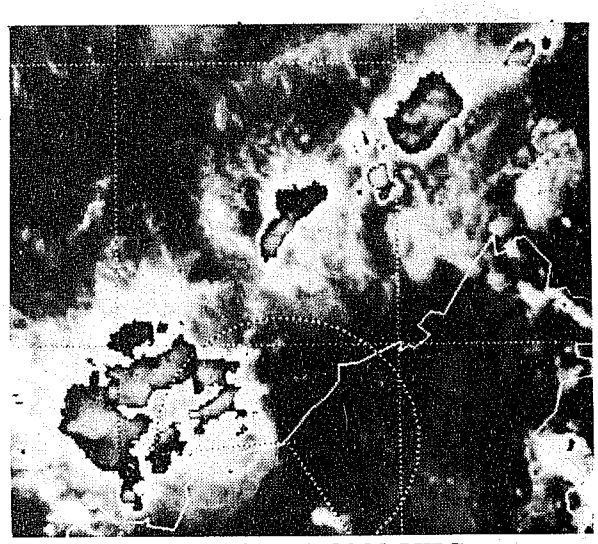

(b) GMS - 1 Infrared 0233 UTC

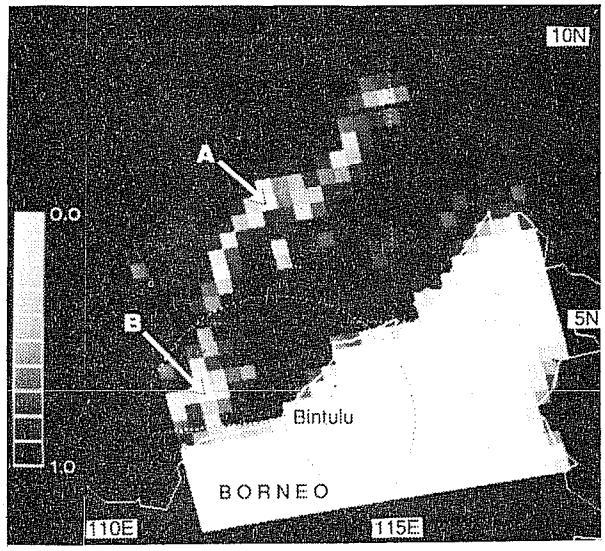

(c) SMMR: 0412 UTC

Figure 6: *Illustration of relationship between operational satellite images (from the GMS-1 geostationary satellite) Nimbus 7 SMMR measurements of rain (or ICLW) and radar intensity, for December 11, 1978 (after Petty and Katsaros, 1988).*
a) GMS-1 Visible 0233 UTC.
b) GMS-1 Infrared 0233 UTC.
c) SMMR: 0412 UTC.
d) GMS-1 Visible 0533 UTC.
e) GMS-1 Infrared 0533 UTC.

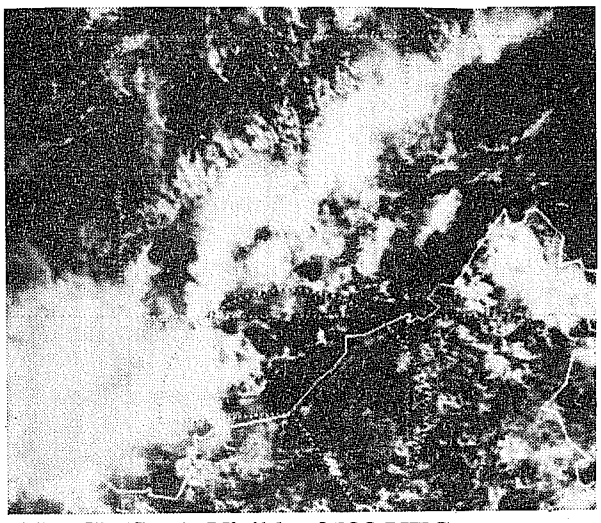

(d) GMS - 1 Visible 0533 UTC

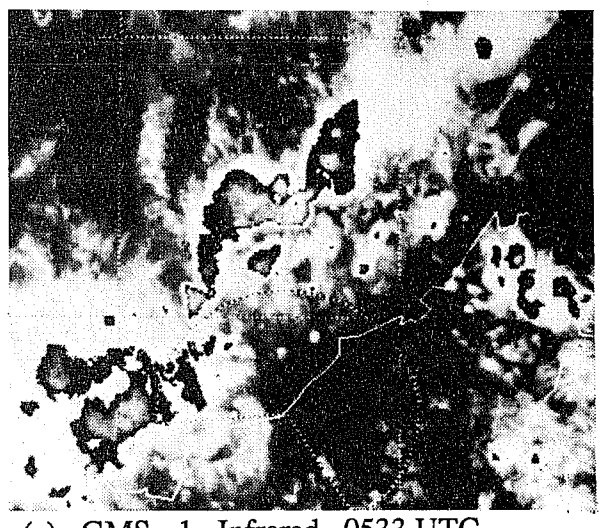

(e) GMS - 1 Infrared 0533 UTC

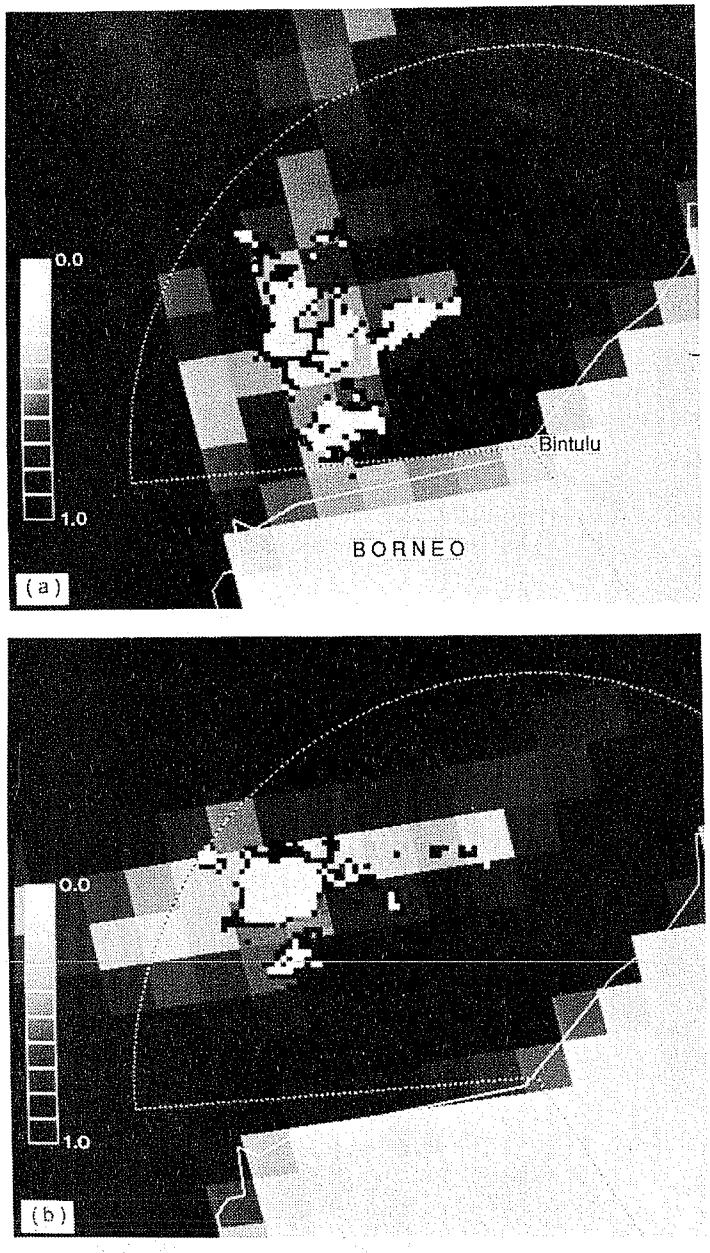

Figure 7: *Observed radar patterns overlayed on coincident SMMR normalized polarization pattern. Dashed arc represents range of 256 km from radar site at Bintulu. Black radar pixels represent echoes exceeding the minimum detectable signal; white pixels represent values exceeding 20 dBZ (after Petty and Katsaros, 1988).*

a) 11 December cloud cluster:: radar data from 0407 UTC; SMMR data from 0412 UTC.

b) 23 December cloud cluster: radar data from 0410 UTC; SMMR data from 0415 UTC.

From the SMMR water vapor and rain fields one could infer that much stronger surface convergence (and therefore greater vertical velocity) would be required to produce the observed same rain rate in the region of the low pressure center as along the cold front (at 37°N, 50°W) since the IWV content is lower by a factor of two at the low center than at the cold front, Figure 8a, b. Figure 8c, which shows contours of divergence calculated from scatterometer wind vectors confirms this deduction. The surface convergence is greater by a factor of two or three at the low pressure center.

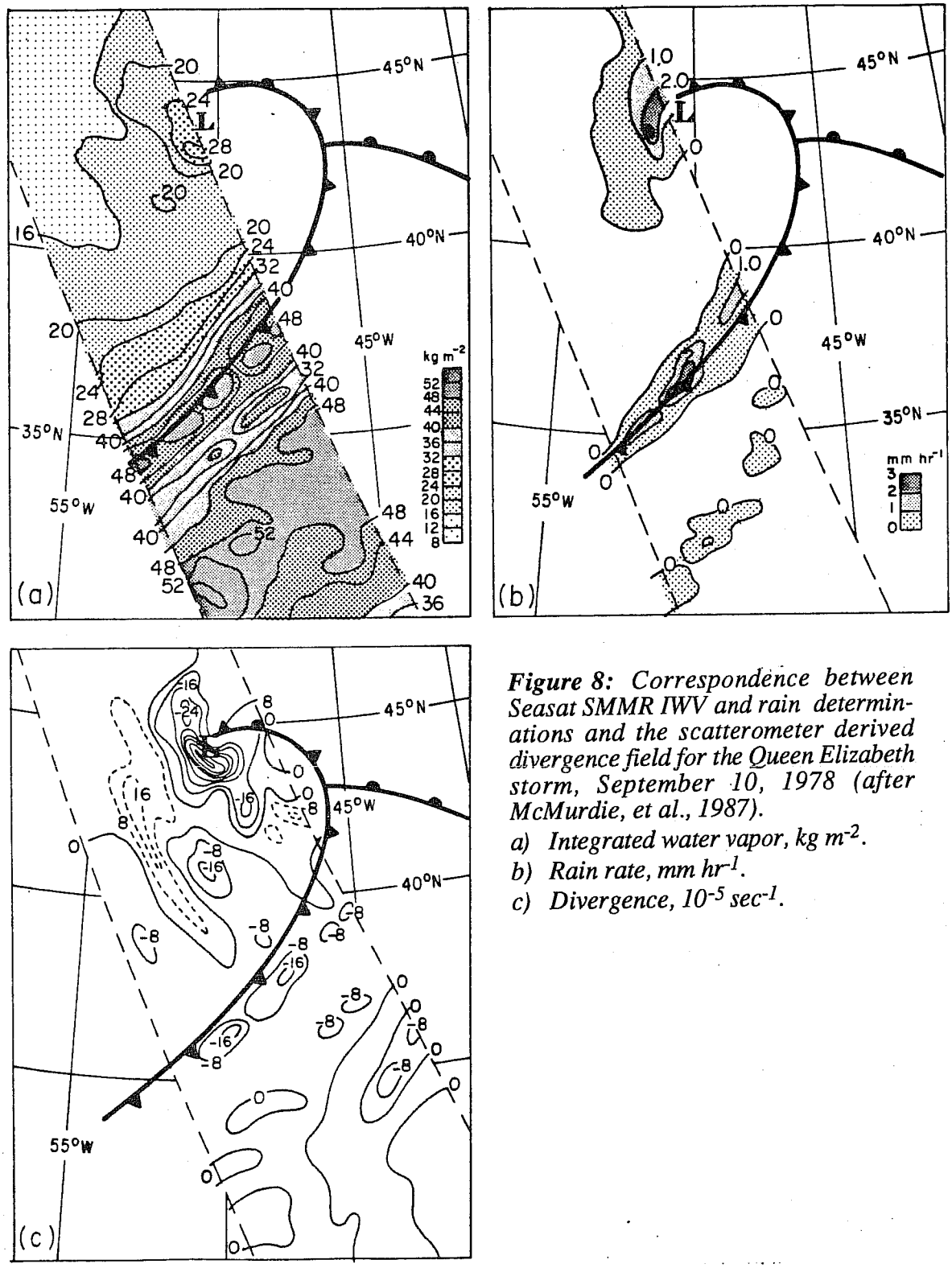

Figure 8: *Correspondence between Seasat SMMR IWV and rain determinations and the scatterometer derived divergence field for the Queen Elizabeth storm, September 10, 1978 (after McMurdie, et al., 1987).*

a) Integrated water vapor, kg m^{-2}.

b) Rain rate, mm hr^{-1}.

c) Divergence, 10^{-5} sec^{-1}.

As we gain confidence in the algorithms for parameters derived from scatterometers and microwave radiometers, a synergy in interpretation occurs when fields of these parameters are used together. Perhaps, one could even estimate net vertical velocities in the lower atmosphere, albeit rather crudely (McMurdie et al., 1987). Further synergy could

undoubtedly be achieved with visible and infrared data providing estimates of cloud-top height and cloud depth.

6. RAIN AND INTEGRATED WATER VAPOR FROM SMMR AND FROM NUMERICAL MODELS

6.1 Limited Area Models

Recently the hydrologic cycle has been given more realistic formulations in Limited Area Numerical Models (LAM's) with grid-resolution of 40 to 80 km (Hammarstrand, 1987; Sundqvist, 1978; Anthes et al., 1987). None of the parameters can be readily verified over large areas of the oceans with conventional data. However, water vapor can be checked against radiosonde ascents from weather ships or island stations. Cloud liquid water is an important parameter, particularly for the radiative balance in the model, so the possibility of obtaining direct measures of this quantity from microwave instruments on satellites has been welcomed by modelers. However, finding coincident model runs with SMMR data over a storm required some patience, particularly since the Nimbus 7 SMMR was only "on" every other day and computer runs of LAM's require initialization from global models such as ECMWF's. Some promising first comparisons were reported by Katsaros et al. (1988); one case is shown in Figure 9.

The cloud physics in the model of Hammarstrand (1987) differentiates between stratiform and cumulus convection. One can infer from Figure 9 that the model appears to have made a realistic choice in this regard, when compared to SMMR rain plots produced with the polarization based algorithm of Petty and Katsaros (1988). However, for the same case the values of integrated water vapor in the model are too large. Because of the narrow swath of SMMR it is impossible to check if compensating drier air was produced elsewhere.

Obviously, SMMR can aid the modeler in evaluating how well the model mimics the macrophysical properties of clouds. By the evolution, location and advection of such areas the dynamics of the model are also tested. A more proper test of the model would be to initialize it with directly measured water vapor and cloud fields.

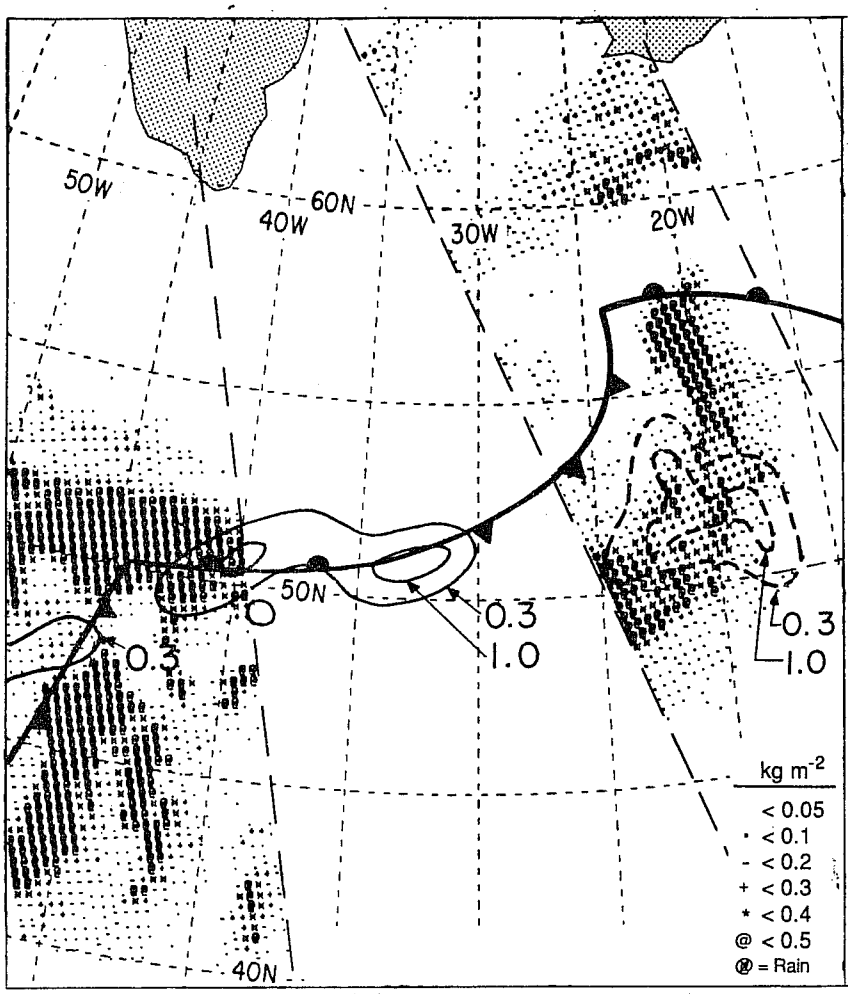

Figure 9: *SMMR-inferred integrated liquid water content (ILWC) observed over the North Atlantic at 1218 UTC (right swath) and 1358 UTC (left swath), 23 May 1983, compared with accumulated precipitation (mm) predicted by Sundqvist-Hammarstrand limited-area model for period 23 May, 00 UTC - 23 May, 18 UTC. Values of SMMR ILWC > 0.5 kg m^{-2} are interpreted as rain of unknown intensity. Solid contours represent stratiform precipitation predicted by model; dashed contours represent convective precipitation. Frontal positions correspond to routine National Meteorological Center analysis, valid 12 UTC (after Katsaros et al., 1988).*

Perhaps this will eventually be possible with the better coverage both in time and space from the SSM/I.

Similarly, a computer calculation of rain with the NCAR (National Center for Atmospheric Research) model (Anthes et al., 1987) for the QE II storm at the stage presented in Figure 8 shows very realistic distribution of the rain regions, including the occurrence of a secondary rain band S.E. of the cold front (Figure 10). Only qualitative comparison is possible at present, since the model does not specifically produce rain rate. The SMMR signals are, actually, also indicative of the liquid water in the column. Whether these water droplets are, in fact, falling out cannot be directly sensed by a passive microwave instrument.

6.2 Interpretation of SMMR Fields with the FGGE Data Set

Because so few other data exist to compare to SMMR fields, the numerical model fields of the FGGE data set have been employed in a Ph.D. thesis by McMurdie (1988) to analyze

mid-latitude cyclones and interpret the information available from SMMR. The following observations have been made: The FGGE data, because of their coarse resolution, carry too much moisture in frontal regions (Figure 11) but maximum and minimum values are quite realistic. Calculated trajectories for parcels arriving ahead of and behind cold fronts illustrate that advection rather than local convergence is mainly responsible for the large amount of moisture in the warm sector ahead of cold fronts and for contrasting dryness behind (see Figure 3 also).

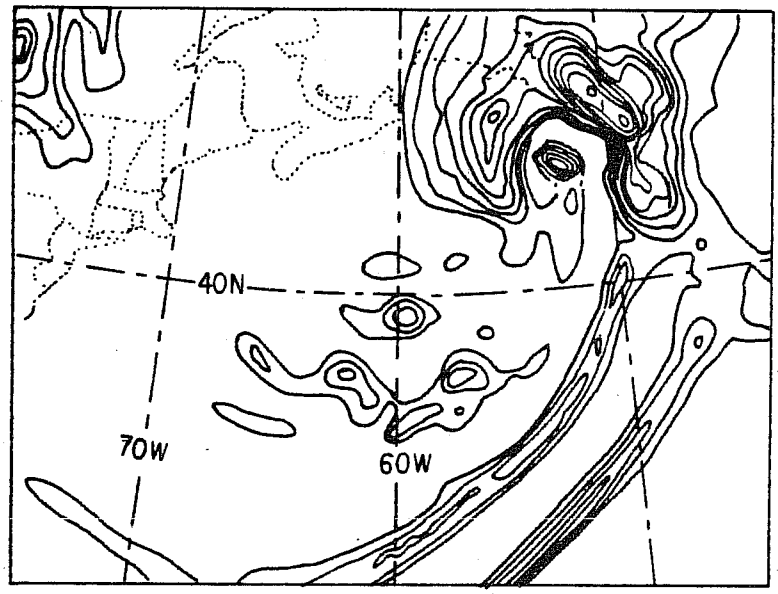

Figure 10: *Cloud liquid water (rain) pattern produced by the Penn-State-NCAR limited area full-physics-model for the "Queen Elizabeth II" storm from a 24-hour forecast valid at 12 UTC, 10 September, 1978. Units on contours are not labeled since quantitative comparison is not attempted here (Courtesy Y.-H. Kuo.) Compare Figure 8b, which shows the Seasat SMMR rain rate pattern for the same time and location.*

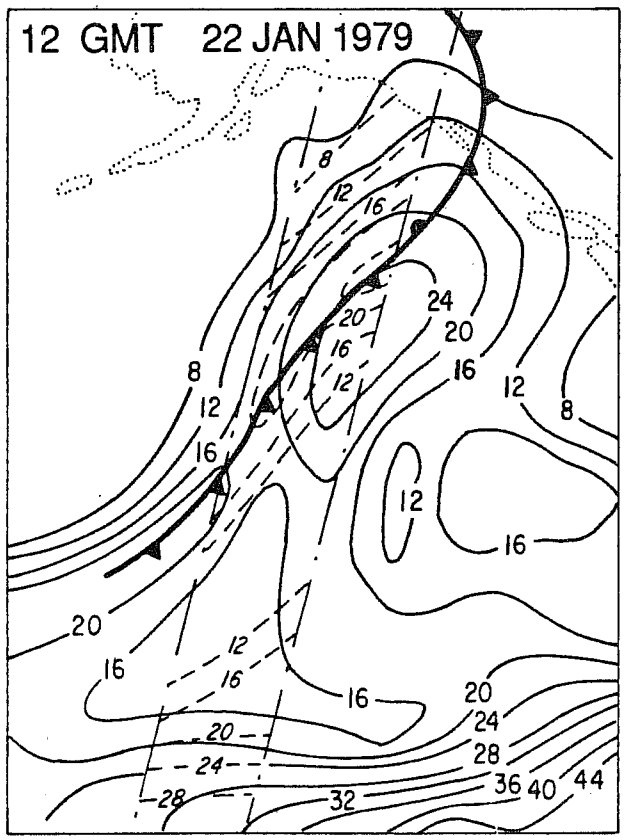

Figure 11: *Comparison of SMMR and FGGE derived integrated water vapor (in kg m^{-2}) for 12 GMT 22 January, 1979 in the North Pacific.*
——— FGGE; ----- SMMR.
The SMMR information lies between the dash-dot lines outlining the SMMR overpass (after McMurdie, 1988).

7. CONCLUSIONS AND A LOOK TO THE FUTURE

We have seen above that microwave measurements of integrated water vapor, cloud liquid water and rain over the ocean offer valuable new data sources for observing the atmospheric water in mid-latitude cyclones and tropical cloud clusters. The ability to estimate cloud liquid water and rain directly is the unique property of microwave radiometry. Our first concern in future work should, therefore, be to test existing algorithms and to continue to improve their formulations. Since there are few other sources of data on cloud liquid water content, one avenue for testing algorithms is by comparing to the products of limited area models with physically based cloud water and precipitation routines. Since these routines have been tested over land and the output has to be consistent with other parameters in the model, this procedure has some validity. However, the modelers are looking to the remote sensing scientists for verification of their cloud water and precipitation routines. This kind of collaboration is known as "the bootstrap" method and is not totally satisfying. However, used judiciously, it can provide the needed information for improvement in both models and satellite algorithms, and should eventually allow greater confidence in both models and satellite data.

Another avenue for verification of satellite algorithms is to participate in field projects, where the appropriate measurements are made *in-situ* from aircraft or from surface based radars or radiometers. Such opportunities have presented themselves in the First ISCCP Regional Experiment (FIRE), where ISCCP stands for International Satellite Cloud Climatology Project, aimed at understanding the stratus clouds west of the southern California coast. It took place in June-July 1987. The Ocean Storms Experiment over the Eastern North Pacific Ocean and the FRONTS '87 experiment in the region between France, England and Ireland, were both studies of mid-latitude cyclones. A future one is the Experiment on Rapidly Intensifying Cyclones in the Atlantic (ERICA), which is planned for late 1988, early 1989 in the Western North Atlantic Ocean.

We have only scratched the surface of the possibilities for using combinations of satellite data of different kinds to interpret the dynamic and thermodynamic state of the atmosphere.

SMMR and scatterometer synergy was described above. No scatterometer is currently in space, but several are planned, notably the one on the European Satellite, ERS1, scheduled for launch in 1990. Currently, an altimeter on the U.S. GEOSAT Satellite provides subtrack winds, which can be combined with radiometer data from SSM/I to locate fronts. This research is under way (with collaborator N. Mognard).

Our bounded imagination, substantial inertia in the system and lack of organization limit us at present from taking full advantage of multi-sensor synergy. Mismatch between areal coverage and resolution of different sensors and the uncoordinated sampling from different satellites hinders research to develop strategies for full use of a multi-faceted satellite view of the earth's atmosphere. The ability of ECMWF global analyses to tie information together may be helpful in this regard, especially when the planned higher resolution of the model is implemented.

At present the SSM/I on the DMSP satellite gives us an opportunity to further some of these ideas. In addition to the combination with limited area models and altimeter studies mentioned above, this instrument will provide another view of cloud systems, not available before, thanks to ice-sensitive channels at 85 GHz. Visible and infrared instruments are present on the same satellite and provide high resolution images. Unfortunately, digital data from these instruments are not archived routinely. Some sample studies should be carried out with such data to illustrate how visible and infrared radiances can be included in algorithms for analysis of cloud systems. With its continuous operation and double swath width compared to SMMR, this new instrument is a promising improvement.

The future Earth Observing System should be planned with complementary satellite sensors located on the same platform, boresighted together. Identifying the scientific opportunities that such improved data gathering can provide to the meteorological community is an important task for the next few years.

8. ACKNOWLEDGMENTS

This review has benefitted from discussion with Grant W. Petty and Lynn A. McMurdie. The work was supported by NASA Grant No. NAG5-943. The able assistance of Ms. Janet Meadows and Ms. Kay Dewar in production of the text and figures is sincerely appreciated.

9. REFERENCES

Adler, R.F. and A.J. Negi, 1988: A satellite technique to estimate tropical convective and stratiform rainfall. *J. Appl. Met.*, **27**, 30-51.

Alishouse, J.C.,1983: Total precipitable water and rainfall determinations from the Seasat Scanning Multichannel Microwave Radiometer (SMMR). *J. Geophys. Res.*, **88**, 1929-1935.

Anthes, R.A., Hsie, E-Y. and Y-H. Kuo, 1987: Description of the Penn State/NCAR Mesoscale Model Version 4 (MM4). National Center for Atmospheric Research, P.O. Box 3000, Boulder, CO 80307.

Born, G.H., J.A. Dunne and D.B. Lame, 1979: Seasat mission overview. *Science*, **204,** 1405-1406.

Buettner, K.J.K., 1963: Regenortung von Wettersartelliten mit Hilfe von Zentimeterwellen. *Die Naturwissenschaften,* **50**, 591-592.

Chang, H.D., P.H. Hwang, T.T. Wilheit, A.T.C. Chang, D.H. Staelin and P.W. Rosenkranz, 1984: Monthly distributions of precipitable water from the Nimbus 7 SMMR data. *J. Geophys. Res.*, **89**, 5328-5334.

Deirmendjian, D., 1963: Complete Microwave Scattering and Extinction Properties of Polydispersed Cloud and Rain Elements. The Rand Corporation, Santa Barbara, CA. R-422-PR.

Deirmendjian, D., 1968: Electromagnetic Scattering on Spherical Polydispersions. Elsevier Press, New York, 290 pp.

Gloersen, P.D. and F.T. Barath, 1977: A Scanning Multichannel Microwave Radiometer for Nimbus-G and Seasat-A. *IEEE J. Ocean. Eng.*, QE2, 172-178.

Gloersen, P.D., D.J. Cavalieri, A.T.C. Chang, T.T. Wilheit, W.J. Campbell, O.M. Johannessen, K.B. Katsaros, K.F. Kunzi, D.B. Ross, D. Staelin, E.P.L. Windsor, F.T. Barath, P. Gudmandsen, E. Langham and R.O. Ramseier, 1984: A Summary of Results from the First Nimbus-7 SMMR Observations. *J. Geophys. Res.*, **89**, 5335-5344.

Hammarstrand, U., 1987: Prediction of Cloudiness Using a Scheme for Consistent Treatment of Stratiform and Convective Condensation and Cloudiness in a Limited Area Model. Special Volume of the J. Met. Soc. Japan. Short- and Medium-range Numerical Weather Prediction. Collection of papers presented at the WMO/IUGG NWP Symposium, Tokyo, 4-8 August, 1986, 187-197.

Hollinger, J., R. Lo, G. Poe, R. Savage and J. Pierce, 1987: Special Sensor Microwave/Imager User's Guide. Naval Research Laboratory, Washington, D.C., 177 pp.

Katsaros, K.B., P.K. Taylor, J.C. Alishouse and R.J. Lipes, 1981: Quality of Seasat Scanning Multichannel Microwave Radiometer (SMMR) Atmospheric Water Determinations. In Oceanography From Space, edited by J.F.R. Gower, pp. 691-706, Plenum, New York.

Katsaros, K.B. and R.M.Lewis, 1986: Mesoscale and synoptic scale features of North Pacific weather systems observed with the Scanning Multichannel Microwave Radiometer on Nimbus 7. *J. Geophys. Res.*, **91**, 2321-2330.

Katsaros, K.B., G.W. Petty and U. Hammarstrand, 1988: Liquid Water and Water Vapor in Mid-Latitude Cyclones Observed by Microwave Radiometry and Compared to Model Calculations. Proceedings of Palmĕn Memorial Symposium, Aug. 29-Sept. 2, 1988, Helsinki, Finland.

Katsaros, K.B., I.A. Bhatti, L.A. McMurdie and G.W. Petty, 1989: Passive Microwave Measurements of Water Vapor Fields and Rain for Locating Fronts in Cyclonic Storms. *Weather Forecasting*, (conditionally accepted).

Levy, G. and R.A. Brown, 1986: A simple, objective analysis scheme for scatterometer data. *J. Geophys. Res.*, **91**, 5153-5158.

McMurdie, L.A. and K.B. Katsaros, 1985: Atmospheric water distribution in a midlatitude cyclone observed by the Seasat Scanning Multichannel Microwave Radiometer. *Mon.Wea.Rev.*, **113**, 584-598.

McMurdie, L.A., G. Levy and K.B. Katsaros, 1987: On the relationship between scatterometer derived convergences and atmospheric moisture. *Mon.Wea. Rev.*, **115**, 1281-1294.

McMurdie, L.A., 1988: Interpretation of Integrated Water Vapor Patterns in Oceanic Midlatitude Cyclones Derived from the Scanning Multichannel Microwave Radiometer. Ph.D. Thesis. Dept. of Atmospheric Sciences, University of Washington, Seattle, WA 98195.

Olson, W.S., 1987: Estimation of rainfall rates in tropical cyclones by passive microwave radiometry. Ph.D. dissertation, University of Wisconsin, Madison, 282 pp.

Petty, G.W. and K.B. Katsaros, 1988: Precipitation Observed over the South China Sea by the Nimbus 7 Scanning Multichannel Microwave Radiometer during Winter MONEX. *J. Appl. Meteor.*, (submitted).

Spencer, R.W., B.B. Hinton and W.S. Olson, 1983a: Nimbus-7 37 GHz radiances correlated with radar rain rates over the Gulf of Mexico. *J. Clim. Appl. Meteor.*, **22**, 2095-2099.

Spencer, R.W., B.B. Hinton and J.A. Weinman, 1983b: Satellite microwave radiances correlated with radar rain rates over land. *Nature*, **304**, 141-143.

Spencer, R.W., W.S. Olson, W. Rongzhang, D.W. Martin, J.A. Weinman and D.A. Santek, 1983c: Heavy thunderstorms observed over land by the Nimbus 7 scanning multichannel microwave radiometer. *J. Clim. Appl. Meteor.*, **22**, 1041-1046.

Spencer, R.W., 1984: Satellite passive microwave rain rate measurement over croplands during spring, summer and fall. *J. Clim. Appl. Meteor.*, **23**, 1553-1562.

Spencer, R.W. and D.A. Santek, 1985: Measuring the global distribution of intense convection over land with passive microwave radiometry. *J. Clim. Appl. Meteor.*, **24**, 860-864.

Spencer, R.W.,1986: A satellite passive 37 GHz scattering-based method for measuring oceanic rain rates. *J. Clim. Appl. Meteor.*, **25**, 754-766.

Staelin, D.H., K.F. Kunzi, R.L. Pettyjohn, R.K.L. Poon, R.W. Wilcox and J.W. Waters, 1976: Remote sensing of atmospheric water vapor and liquid water with the Nimbus-5 microwave spectrometer. *J. Appl. Meteorol.*, **15(11)**, 1204-1214.

Sundqvist, H., 1978: A parameterization scheme for non-convective condensation including prediction of cloud water content. *Quart. J. Roy. Met. Soc.*, **104**, 677-690.

Taylor, P.K., K.B. Katsaros and R.G. Lipes, 1981: Determination by Seasat of atmospheric water and synoptic fronts. *Nature*, **294**, 737-739.

Taylor, P.K., T.H. Guymer, K.B. Katsaros and R.G. Lipes, 1983: Atmospheric Water Distributions Determined by the Seasat Multichannel Microwave Radiometer. In Variations in the Global Water Budget, edited by A. Street-Perrot, M. Beran and R. Ratcliffe, pp. 93-106, D. Reidel Publishers, Dordrecht, Holland.

Wilheit, T.T. and A.T.C. Chang, 1980: An algorithm for retrieval of ocean surface and atmospheric parameters from the observations of the scanning multichannel microwave radiometer. *Radio Science*, **15**, 525-544.

Wilheit, T.T., A.T.C. Chang, M.S.V. Rao, E.B. Rodgers and J.S. Theon, 1977: A satellite technique for quantitatively mapping rainfall rates over the oceans. *J. Appl. Meteor.*, **16**, 551-560.

Woiceshyn, P.M., M.G. Wurtele, D.H. Boggs, L.F. McGoldrick and S. Petherych, 1986: The necessity for a new parameterization of an empirical model for wind/ocean scatterometry. *J. Geophys. Res.*, **91**, 2273-2288.

Wurtele, M.G., P.M. Woiceshyn, S. Peteherych, M. Barowski and W.S. Appleby, 1982: Wind direction alias removal studies of SEASAT scatterometer derived winds. *J. Geophys. Res.*, **87**, 3365-3377.